




# A guiding teaching and dual adversarial learning framework for a single image dehazing

Zhengyun Fang<sup>1</sup> · Ming Zhao<sup>2</sup> · Zhengtao Yu<sup>3,4</sup>  · Meiyu Li<sup>2</sup> · Yong Yang<sup>2</sup>

Accepted: 28 May 2021 / Published online: 11 June 2021

© The Author(s), under exclusive licence to Springer-Verlag GmbH Germany, part of Springer Nature 2021

## Abstract

In most existing deep learning-based image dehazing methods, the haze-free source images are only used as the ground truth for the design of the loss function, whereas the guiding role that the source image should play on different feature levels has been ignored. This will result in a sub-optimal dehazing output. To address this issue, inspired by the knowledge distillation, a guiding teaching framework is designed for single image dehazing in an end-to-end manner, where the features of the haze-free source image at different levels are completely used to promoting the restoration of the hazy image. Specifically, the framework consists of a two-stream convolutional neural network termed teacher stream (TS) and student stream (SS), respectively. The input of the former is a haze-free image while the output is the desired image after reconstruction. The input of the latter is the hazy image, and the output is the restored image. Moreover, a dual adversarial strategy is designed to further improve the ability of SS to imitate teacher stream. In this process, the output results of SS are divided into two categories according to their hazy intensity levels. Then a thick light discriminator is introduced and made against the SS pit, such that the images with better dehazing effects can be used to deal with the ones poorly dehazed. A second discriminator termed light clear discriminator (LCD) is further introduced and a minimax game between the LCD and the SS is defined to drive the final result produced by SS closer to the reconstruction result of the TS. Experimental results show that the proposed method outperforms several latest methods applied to both artificial hazy images and the hazy images from the real scene.

**Keywords** Image dehazing · Knowledge distillation · Adversarial learning · Teacher stream · Student stream

## 1 Introduction

Haze is a common factor that affects the outputs of computer visual tasks. It is formed either by dust, smoke, small particles floating in the air or by the fog evaporated from the liquid. Its appearance significantly affects the visual tasks such as target recognition, satellite positioning and image classifica-

tion. Therefore, the dehazing techniques play a crucial role in the development of computer vision.

The present image dehazing methods mainly include prior knowledge-based methods and learning-based methods. A prior knowledge-based method refers to the use of additional prior information as compensation for the damaged image to achieve image dehazing effect [16,22,31,31,38,51,69,71]. Particularly, He et al. [16] proposed a haze removal method based on dark channel prior knowledge. This method, however, does not perform sufficiently under the bright sky. In the work of Khmag et al. [22], the second-generation wavelet transforms and the mean vector l2-norm for single image dehazing are developed, where the mean vector l2-norm is used to estimate the transmission map, and the second-generation wavelet transform is used to enhance the estimated transmission map in order to improve the visual quality of the resulted image. However, for a two-dimensional transmission map, the second-generation wavelet transform is not optimal, which limits the further improvement of the final quality. Meng et al. [38] proposed a single image dehaz-

---

✉ Zhengtao Yu  
ztyu@hotmail.com; ztychina99@126.com

<sup>1</sup> College of Land Resource Engineering, Kunming University of Science and Technology, Kunming 650500, China

<sup>2</sup> Electric Power Research Institute of Yunnan Power Grid Co., Ltd., Kunming 650217, China

<sup>3</sup> Faculty of Information Engineering and Automation, Kunming University of Science and Technology, Kunming 650500, China

<sup>4</sup> Yunnan Key Laboratory of Artificial Intelligence, Kunming University of Science and Technology, Kunming 650500, China

ing approach based on boundary constraints and  $l_1$  norm weighted context regularization constraints. In this method, a group of filters is introduced in the dehazing process to reduce image noise and enhance the main structure and detail information of the image after dehazing. Furthermore, based on the prior knowledge of the atmosphere transfer map, Li et al. [31] proposed the local smoothness of the atmospheric transfer map and the non-statistically independent prior to the scene albedo. The author also made an assumption that the atmospheric transfer map is greater than the scene absorption rate. The objective function model was then built and the images were dehazed based on the prior knowledge and assumptions. This kind of method can only achieve the dehazing effect to a limited extent since its original performance is highly dependent on the assumptions, which can be invalid for specific images or the prior knowledge is unreliable.

Different from prior knowledge-based dehazing methods, the learning-based methods use a network trained under deep learning frameworks to achieve the desired result. There are two classic types of learning-based approaches:

*The methods based on the atmospheric scattering model* In this kind of models, the transmission map and global atmospheric light are estimated by a deep learning network [42, 61, 66]. For example, Ren et al. [42] proposed a multi-scale convolutional neural network (MSCNN), through which the transmission map was learned by a complete convolution network. This approach consists of a fine-scale net, where the coarse-scale net is used to predict a holistic transmission map and the fine-scale net is used to refine the results locally. This method only calculates the difference between the recovered image and the ground truth image in model training. Zhang et al. [61] proposed an end-to-end densely connected pyramid dehazing network (DCPDN), which learned transmission map, atmospheric light and dehazing image. This method used an encoder–decoder to learn multi-scale features in a multi-level pyramid pool module. However, the experimental results show that the performance of this method is not satisfactory in real hazy images because of its weak generalization ability. Some works approached the dehazing problem by learning the transmission map [4, 22, 56, 63]. Nevertheless, the estimation accuracy on the transmission map and atmospheric light still remains to be improved and the dehazing effect is limited.

*The methods that use the deep convolutional neural network directly to restore a clear image* This kind of approach is essentially an end-to-end method [7, 26, 32, 34, 43, 57, 64, 65]. Liu et al. [34] proposed to study the internal propagation behavior of deep networks based on energy change and built a lightweight learning framework to train the network for dehazing. This method integrated the advantages of prior driven models and data-driven networks and avoided the limitations of the existing dehazing approaches. Li et al. [26]

proposed an integrated dehazing network based on a convolutional neural network, which unified the transmission map estimation and global atmospheric light estimation into one variable, so as to reduce the complexity of network structure. However, the inaccurate estimation of transmission map and global atmospheric light may produce a cumulative error, which would compromise the quality of the dehazing results. Ren et al. [43] proposed a multi-scale threshold fusion network to effectively increase network receptive field and reduce aperture effect. This method can avoid the introduction of halo artifacts, but the computational efficiency is degraded. Li et al. [32] put forward a dehazing method based on conditional generative adversarial nets (CGAN) and solved the problems of dark channels, color differences and maximum contrast in the priority-based method. Swami et al. [48] realized the image dehazing by conditional adversarial networks (CAN). Since the image fusion can synthesize the information of different images [28–30, 54, 68], Guo et al. [14] developed a deep convolutional network for a single image dehazing based on derived image fusion strategy. In the above-mentioned deep learning-based methods, the haze-free source image is usually used in the design of loss functions as ground truth. This kind of design method fails to fully exploit the guiding effect of a haze-free clear image, so it is easy to produce sub-optimal dehazing results.

To tackle the current problems existing in the end-to-end method, we propose a new end-to-end guiding teaching framework. Specifically, our framework consists of two streams with different tasks, i.e., the teacher stream (TS) and the student stream (SS). The TS is a reconstruction sub-network, and the SS is a dehazing sub-network, which share the same structure. The input of TS is the haze-free source image, and its output is the reconstructed clear image that has the same content as the input image. The input of SS is the hazy version of the same haze-free source image whose output is a clear image after restoration. The goal is to leverage the performance of the dehazing sub-network under the guidance of clear images. To this end, the SS is thus guided to extract the same features with that of the TS, as long as the inputs of both streams are paired images. The proposed method regularizes the feature learning at different layers, whereas the convolutional neural network-based methods only use the clear source image as ground truth to design the loss functions. To further improve the quality of the dehazing image, a novel dual adversarial strategy is developed to boost up the ability of SS to imitate the TS. The outputs of the SS are categorized into two types according to their hazy intensity levels. Then a thick light discriminator (TLD) is introduced and made against the SS pit, such that the images with better dehazing effects can be used to deal with the ones poorly dehazed. A second discriminator termed light clear discriminator (LCD) is further introduced and a mini-max game between LCD and SS is defined to drive the final

result produced by SS closer to the clear labeled image. This mutual assistance mode is very conducive to improve the dehazing quality of different images. The proposed method is inspired by the latest advances in the knowledge distillation [12,13,17,19,40,53]. It is simple and effective for a single image dehazing. The main contribution of this work is summarized as follows:

- We develop an end-to-end guiding teaching framework for a single image dehazing. This framework consists of TS and SS, where under the assistance of TS, the guiding effect of hazy-free image can be fully exploited, such that better visual effects of the dehazing result is achieved.
- We propose to divide the output results of SS into two categories according to their hazy intensity. Then a TLD is introduced and made against the SS pit, such that the images with better dehazing effects can be used to deal with the ones poorly dehazed.
- We introduce the second discriminator LCD and a mini-max game between LCD and SS to drive the final result produced by SS closer to the clear labeled image. In our method, the TLD, LCD and SS are jointly optimized under the guidance of TS.

The remainder of the paper is organized as follows. Section 2 reviews the state-of-the-art methods related to this work. The proposed approach is presented in detail in Sect. 3. Then the experiments are conducted and the results are discussed in Sect. 4. Finally, the work is concluded in Sect. 5.

## 2 Related work

### 2.1 CNN-based image dehazing

CNN is essentially an input–output mapping that can learn the mapping relationship between a substantial amount of inputs and outputs without any precise mathematical expressions. CNN is extensively used in the fields such as image classification [11], target detection/recognition [1], image enhancement [15] and image dehazing [49]. For image dehazing, Tang et al. [49] proposed to obtain the dehazing image by directly mapping the hazy image to its corresponding haze-free image. However, due to the lack of the constraints of clear image features, the visual effect after the dehazing is not ideal. Chen et al. [5] introduced a gated context aggregation into CNN to directly recover the final haze-free image. In their work, the smoothed dilation technique is used to suppress the gridding artifacts caused by the dilated convolution, but the gridding artifacts cannot be eliminated. By adding an extra layer to the traditional CNN, Song et al. [47] realized the extraction of statistical attributes for single image dehazing. This approach has certain achieve-

ments both in terms of subjective and objective evaluation, yet it only extracts the attribute of contrast ratio and fails to consider other statistical attributes. Dong et al. [9] employed an attention mechanism to sufficiently extract the features to improve the quality of the recovered image but the visual effect of the image is over-enhanced (too bright). To deal with the problems in the above-mentioned methods as well as to achieve a better dehazing effect, an end-to-end CNN guiding teaching framework is therefore proposed to extract features at a different level for the single image dehazing.

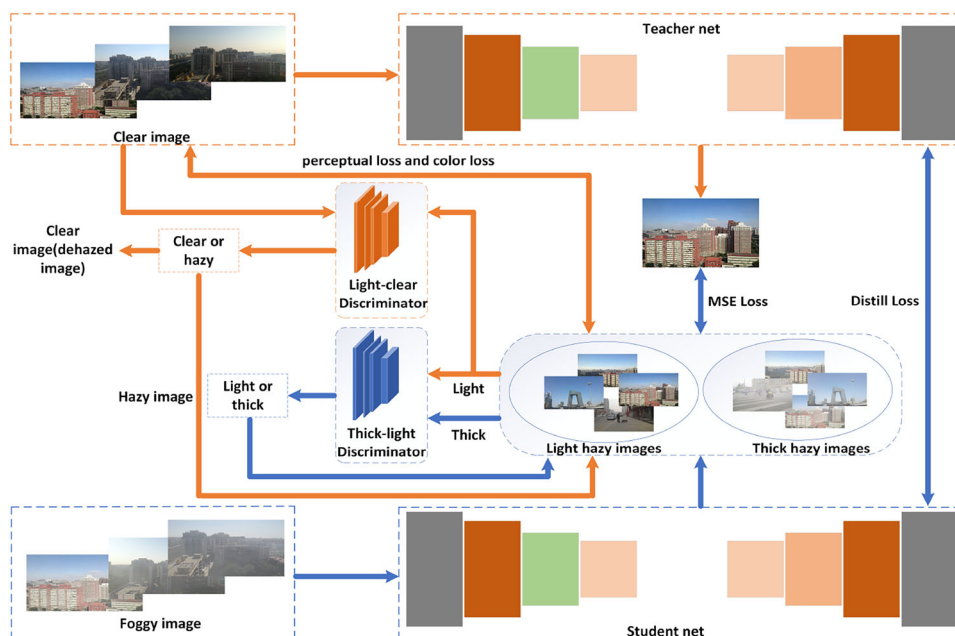
### 2.2 GAN-based image dehazing

GAN has a remarkable potential to generate realistic images and has been applied in various vision tasks, such as super-resolution [24,67], deraining [62], deblurring [23] and denoising [6]. For image dehazing, Yang et al. [58] developed a disentangled dehazing network for generating realistic haze-free images. This method contains three generators for the scene radiance and can alleviate the paired training constraint. Mehta et al. [37] developed a hyperspectral-guided image dehazing generative adversarial network for image dehazing where enhanced versions of CycleGAN [70] and conditional GAN for spatial–spectral spatial mapping are designed. Engin et al. [10] used CycleGAN for image dehazing along with the perceptual loss to generate more visually realistic dehazed images. The GAN-based dehazing methods only make the dehazed image close to the clear image in terms of distribution. In fact, the concentration of haze is not considered in the GAN-based dehazing methods. In the process of adversarial learning, if the training images with different haze concentrations are mixed together, it may have a negative impact on the final dehazing effect. To solve this problem, a novel adversarial learning strategy is proposed, where the outputs of SS are divided into thick and light hazy levels through a predefined threshold.

### 2.3 Knowledge distillation

It has been proved that the performance of network learning can be significantly improved with the deepening of network layers. However, deeper layers will introduce more parameters, which in turn increases the computation burden and raises the storage costs. Therefore, researchers seek alternative ways to achieve compatible results with fewer parameters. Ba et al. [2] studied whether a shallow network can achieve comparable performance with a deep network in 2014. Hinton et al. [18] first proposed and systematically explained the concept of knowledge distillation in 2015. By feature matching in the softmax layer and using the output of softmax to supervise learning, distillation temperature was added to the softmax layer to improve the distillation performance. By adding loss directly in the middle layer, Romero

**Fig. 1** Proposed framework for image dehazing



et al. [44] obtained knowledge by learning the feature maps of the intermediate layers of a deep network, i.e., the TS. It is found that a smaller deep network can deliver better results than the teacher network. By resorting to the attention mechanisms, Zagoruyko et al. [60] demonstrated how the SS can focus on the same areas as the teacher network does. Yim et al. [59] defined the FSP Matrix to describe the characteristic relationship between layers to achieve knowledge transfer. To avoid the over-fitting caused by hard labels and to enhance generalization caused by soft labels, Yang et al. [55] reduced the accuracy of teacher networks to a certain extent to allow student stream with a higher tolerance of extensive learning. The idea of knowledge distillation is thus chosen in this paper for image dehazing.

### 3 Proposed approach

Inspired by knowledge distillation, a guiding teaching and dual adversarial learning framework for a single image dehazing is developed. The network structure is shown in Fig. 1.

The hazy image and its clear source image are fed into the SS and the TS, respectively. The features of the clear image are learned in the TS and are used to guide the SS to learn the features of the haze-free image from the input image. The SS realizes the image dehazing through feature reconstruction. Moreover, a dual adversarial strategy is designed to optimize the image quality after dehazing. The proposed dehazing network can adapt to different hazy levels. In this process, two discriminators are used to improve performance. Specifically, the TLD is used to distinguish the image with

different hazy levels (i.e., thick or light) of the student network output. The LCD is used to distinguish the clear image reconstructed by the teacher network so that they can spit against each other to make the output of the student network closer to the clear image. By introducing the adversarial loss of TLD and LCD, the dual adversarial module can transfer the heavy hazy images into the light hazy image and further transfer the light hazy images into clear haze-free images. In the proposed distillation network, mean square error (MSE) loss, distillation loss, perceptual loss and color loss are used. MSE loss can make the SS output consistent with that of the TS. Distillation loss forces the features extracted by the TS and the SS from different levels to be consistent. Perceptual loss and color loss constrain the outputs of SS and TS to have similar visual effects.

#### 3.1 Knowledge distillation network

The proposed distillation network mainly includes the feature extraction of the TS and the training of the SS. The function of feature extraction of the TS is to learn from the labeled image to obtain feature information contained in the clear picture and guide the SS to extract more accurate features. The network is based on the U-Net [45], where the teacher sub-network and the student sub-network have the same structure. The haze-free images are fed into the TS for supervised training to ensure that the teacher network can reconstruct the clear images. The TS trained can extract the features of the haze-free images. The feature map of each layer obtained in the TS can be described as:

$$F_t(n) = \max(0, W_t(n)X_t(n) + B_t(n)) \quad (1)$$

where  $n \in (1, 2, \dots, N)$  is the number of convolutional layer.  $\mathbf{W}_t(n)$  and  $\mathbf{B}_t(n)$  are the weight and deviation of the  $n$ th convolutional layer, respectively.  $\mathbf{F}_t(n)$  is the feature of the  $n$ th layer extracted by the TS.  $X_t(n)$  is clear labeled image  $X_l$  when  $n = 1$ .  $X_t(n) = \mathbf{F}_t(n - 1)$  if  $n > 1$ .

The hazy images corresponding to the clear images are fed into the SS for feature extraction. The features extracted by the SS can be expressed as:

$$\mathbf{F}_s(n) = \max(0, \mathbf{W}_s(n)X_s(n) + \mathbf{B}_s(n)) \tag{2}$$

where  $n \in (1, 2, \dots, N)$  is the number of convolutional layer.  $\mathbf{W}_s(n)$  and  $\mathbf{B}_s(n)$  are the weight and deviation of the  $n$ th convolutional layer, respectively.  $\mathbf{F}_s(n)$  is the feature of the  $n$ th layer extracted by the SS.  $X_s(n)$  is the input hazy image  $X_h$  when  $n = 1$ .  $X_s(n) = \mathbf{F}_s(n - 1)$  if  $n > 1$ .

The SS training is to take the features of clear images extracted from the TS as guidance and constraint. MSE is used to constrain the distance between two feature maps to achieve a better dehazing. We use knowledge distillation in the SS to obtain more image information from clear images. Note that the purpose of the knowledge distillation in this work is different from that of the traditional distillation which aims to compress network scale and reduce parameters. The purpose is to make the network get more information from clear pictures as labels through knowledge distillation. To eliminate the channel difference of different location feature maps from the TS and the SS, the feature map needs to be converted before its distillation. We use  $1 \times 1$  convolutional layer as convertor  $T$ .  $\mathbf{F}_t(n)$  and  $\mathbf{F}_s(n)$  ( $n \in (1, 2, \dots, N)$ ) denote the  $n$ th layer feature of the TS and the SS, respectively. The distillation loss is defined as:

$$L_{\text{distill}} = \begin{cases} \|\mathbf{F}_t(i) - \mathbf{F}_s(j)\|_1, & \text{if } i = j \\ \|T(\mathbf{F}_t(i)) - T(\mathbf{F}_s(j))\|_1, & \text{otherwise} \end{cases} \tag{3}$$

where  $i$  ( $i \in (1, 2, \dots, N)$ ) and  $j$  ( $j \in (1, 2, \dots, N)$ ) are the distillation location.  $T$  is the conversion network for adjusting the channel number of  $\mathbf{F}_t$  or  $\mathbf{F}_s$ .

In the process of teacher–student network training, the MSE loss, perceptual loss and color loss are used to constrain the output  $\mathbf{Y}$  of the SS to make it as close as possible to the output  $X_c$  of the TS. The MSE loss is described by:

$$L_{\text{MSE}} = \frac{1}{H \times W} \sum_{i=1}^H \sum_{j=1}^W (X_c(i, j) - \mathbf{Y}(i, j))^2 \tag{4}$$

where  $\mathbf{Y}(i, j)$  is the value of the pixel at the position  $(i, j)$  of  $\mathbf{Y}$ ,  $X_c(i, j)$  is the value of the pixel at the position  $(i, j)$  of  $X_c$ .  $H$  and  $W$  are length and width of the image, respectively.

$L_p$  is the perceptual loss [21], which is used to measure the similarity between the dehazed image  $\mathbf{Y}$  and the clear

labeled image  $X_l$ . The perceptual loss is defined as:

$$L_p = \|\phi(\mathbf{Y}) - \phi(X_l)\|_2^2 \tag{5}$$

where  $\phi$  represents the feature maps obtained by 16-layer VGG network.

Besides the MSE loss and perceptual loss, we adopt color loss [20] to solve the problem of color distortion in the output image of defogging network. In this paper, the color loss is formulated as:

$$L_c = \|\mathbf{Y} * \mathbf{G}_s - X_l * \mathbf{G}_s\|_2^2 \tag{6}$$

where  $*$  represents convolution operation.  $\mathbf{G}_s$  is the 2D Gaussian blur operator [20].

### 3.2 Dual adversarial module

There are many discrepancies between hazy and clear images. For example, haze-free images usually have higher contrast and sharper edges compared with hazy images. Most dehazing methods are lying on such priors or assumptions yet they do not hold for all conditions and can be easily intruded in practical. Adversarial learning is commonly used to train the network in literature [6,23,58,62]. The network is divided into two parts: the generator and the discriminator. The input of the generator is the hazy image, and the output is the dehazed image. The input of the discriminator is the dehazing image and the corresponding clear image. The network can extract the information from the hazy image through the adversarial learning between the discriminator and the generator. The discriminator is used to identify whether the input of the network is the dehazed image or the clear image. Meanwhile, the generator output is made as closer as possible to the clear image, so that the discriminator will not distinguish it. Therefore, the network can be used for dehazing.

However, the above-mentioned networks for dehazing use only hazy images and clear image adversarial. In practice, the hazy concentrations in the training dataset are different and the hazy levels thus cannot be neglected. Therefore, we propose dual adversarial learning. In the proposed guiding teaching and dual adversarial learning framework, the SS plays as a generator ( $G$ ). The output of the SS is classified into light hazy and thick hazy images based on their fog density. The discriminators TLD and LCD are trained jointly with the SS. Specifically, the input to the TLD is the two kinds of images of the SS output. The SS is fixed, the TLD is trained, and the TLD adversarial loss is used to constrain the network such that the discriminator can discriminate whether the output of the SS is light hazy or thick hazy. When the SS is being trained, the TLD is fixed and the SS is to confuse the TLD so that the SS can achieve a gradual transition from a thick hazy image to a light hazy image. The light hazy image

of the output of the SS and a clear image are the input of the LCD discriminator. When the LCD is being trained, the LCD adversarial loss is used to constrain the network so that the LCD can discriminate whether its input is light hazy or clear. When the SS is been trained, the LCD is fixed; thus, the SS can achieve a gradual transition from a thick hazy image to a clear image. Finally, the output of the SS is closer to a clear image and achieves the purpose of dehazing.

Fog-aware density evaluator (FADE) [8] is adopted to measure fog density.  $Y$  denotes the output of the SS. The FADE of  $Y$  is compared with the threshold  $\theta$ , which can be preset empirically. Those greater than  $\theta$  are thick hazy images, vice versa. Equations (7) and (8) show the adversarial loss of TLD and LCD, respectively.

$$L_{\text{TLD}} = \min_G \max_D E[\log D(X_{th})] + E[\log(1 - D(X_{lh}))] \quad (7)$$

$$L_{\text{LCD}} = \min_G \max_D E[\log D(X_l)] + E[\log(1 - D(X_{lh}))] \quad (8)$$

where  $X_{th} = G(X_h)$  represents thick hazy image,  $X_{lh} = G(X_h)$  represents light hazy image.  $G$  is the generator, i.e., SS.

The proposed network is trained according to the overall loss function:

$$L_{\text{total}} = L_{\text{MSE}} + L_p + L_c + L_{\text{distill}} + \lambda_1 L_{\text{TLD}} + \lambda_2 L_{\text{LCD}} \quad (9)$$

where  $\lambda_1$  and  $\lambda_2$  are hyperparameters.

For clarity, we summarize the proposed method in Algorithm 1

---

**Algorithm 1** Algorithm of the guiding teaching and dual adversarial learning for image dehazing

---

**Input:** The clear labeled images  $X_l$  and the corresponding hazy images  $X_h$ .

**Initialize:** The hyperparameters  $\lambda_1$  and  $\lambda_2$ , learning rate, the threshold  $\theta$ .

1. Pretraining the teacher network with clear labeled images.
2. Training the SS according to the formula (3), (4), (5) and (6).
3. Training the SS and the discriminator TLD
  - for  $i=1$ :epoch
  - fixing SS, training TLD
  - fixing TLD, training SS
  - end for
4. Training the SS and the discriminator LCD
  - for  $i=1$ :epoch
  - fixing SS, training LCD
  - fixing LCD, training SS
  - end for

**Output:** The trained network.

---

## 4 Experiments

### 4.1 Evaluation criteria

To verify the effectiveness of the proposed method, we evaluate the dehazing results in terms of visual effect and objective indicators. Peak signal-to-noise ratio (PSNR) [36] and Structural Similarity Index (SSIM) [52] are selected as the objective criteria. PSNR can measure the error between the corresponding pixels of the recovered image and its corresponding ideal image. It is an image quality evaluation index based on error sensitivity. SSIM measures the similarity between two images by focusing on the structural information of images and is independent of the brightness, contrast or other image properties. The higher the values of PSNR and SSIM, the better the quality of the recovered result.

Given two images, one is a clear standard image  $X$  and the other is a recovered image  $Y$ , the PSNR can be defined as:

$$\begin{cases} \text{MSE} = \frac{1}{H \times W} \sum_{i=1}^H \sum_{j=1}^W (X(i, j) - Y(i, j))^2 \\ \text{PSNR} = 10 \log_{10} \left( \frac{(2^n - 1)^2}{\text{MSE}} \right) \end{cases} \quad (10)$$

where MSE is the mean square error of standard image  $X$  and result image  $Y$ .  $H$  and  $W$  are the height and width of the image, respectively.  $n$  is the bits of a pixel which is generally set to 8 (i.e., gray level of 256). The unit of PSNR is decibel (dB). A larger value indicates a smaller distortion.

The SSIM is defined as:

$$\text{SSIM}(x, y) = \frac{(2\mu_x\mu_y + c_1)(\sigma_{xy} + c_2)}{(\mu_x^2 + \mu_y^2 + c_1)(\sigma_x^2 + \sigma_y^2 + c_2)} \quad (11)$$

where  $\mu_x$  and  $\mu_y$  are the mean values of  $X$  and  $Y$ , respectively.  $\sigma_x$  and  $\sigma_y$  are the standard deviations of  $X$  and  $Y$ , respectively.  $\sigma_{xy}$  is the covariance of  $X$  and  $Y$ .  $c_1$  and  $c_2$  are set to constants to avoid system error caused by a zero denominator. The value of the SSIM is between 0 and 1. A higher value indicates a smaller difference between the resulting image and the clear image.

### 4.2 Experimental setup

Image dehazing based on deep learning usually needs large-scale training data to train the model. However, it is difficult to collect a large number of hazy images with labels (haze-free images) from a real scene. Moreover, the quality of hazy images and corresponding clear images collected at different times is difficult to control. Therefore, most current dehazing models use the hazy image datasets synthesized from

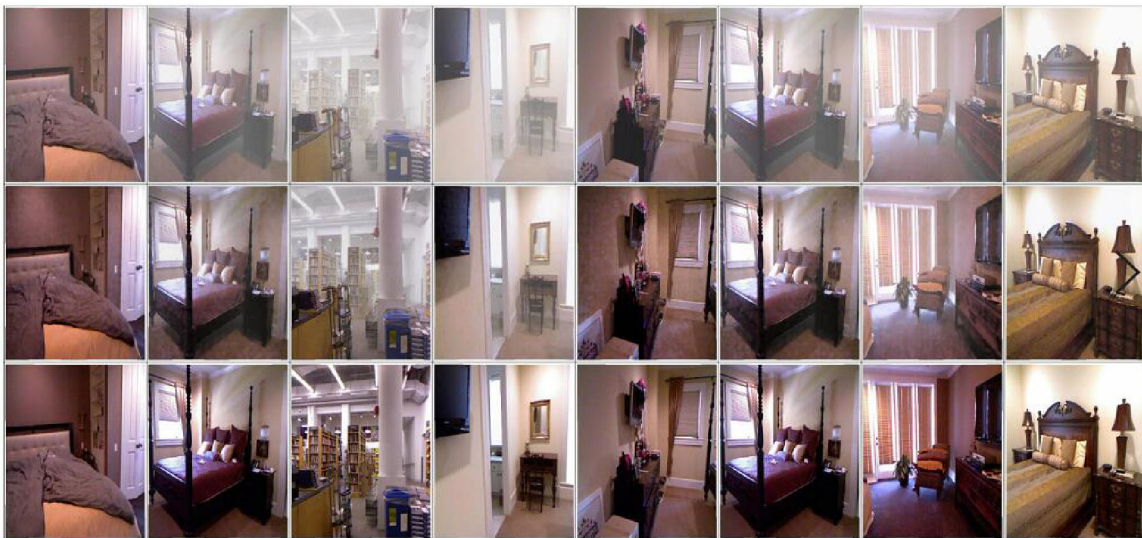


Fig. 2 Dehazing results of the proposed method on synthetic hazy images dataset

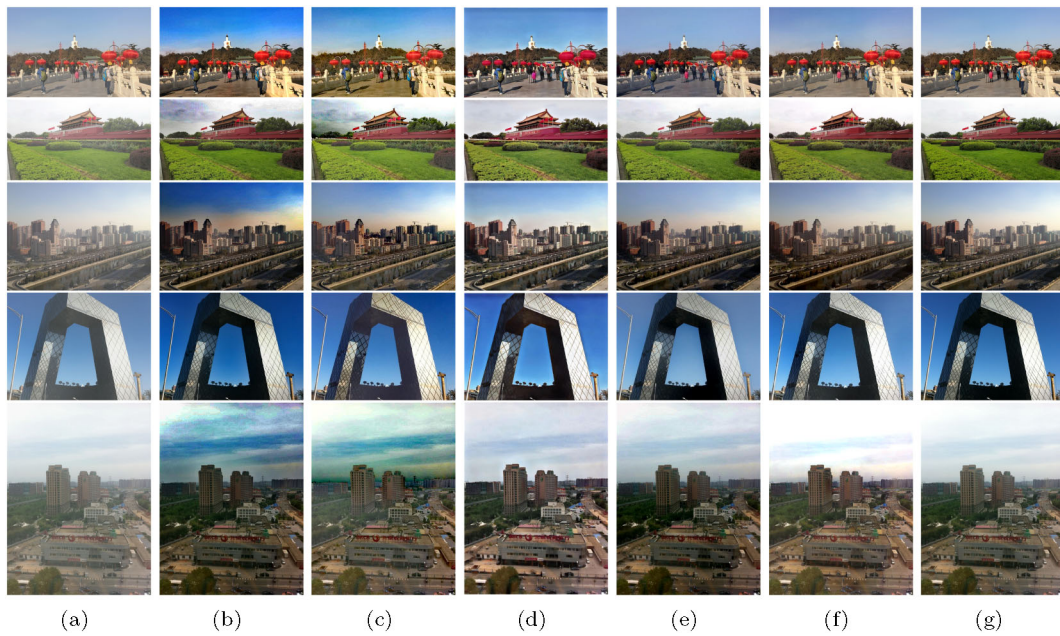


Fig. 3 Comparison of experimental results with different methods. **a** Hazy images, **b** DCP, **c** NLD, **d** DA-Net, **e** DehazeNet, **f** proposed method, **g** ground truth

**Table 1** Evaluation index (PSNR/SSIM) comparison of the dehazing results on synthetic datasets with different methods

Datasets	DCP	DA-Net	DehazeNet	NLD	Ours
TESTSET A	16.61/0.8540	25.78/ <b>0.9221</b>	19.89/0.8351	16.27/0.7918	<b>28.65/0.9105</b>
TESTSET B	19.14/0.8605	27.58/ <b>0.9337</b>	21.44/0.8534	18.32/0.8223	<b>29.38/0.9332</b>
TESTSET C	18.54/0.8337	25.78/0.8921	18.96/0.7753	16.76/0.7356	<b>27.38/0.9182</b>



**Fig. 4** Comparison of experimental results with different methods. **a** Hazy image, **b** DCP, **c** NLD, **d** DA-Net, **e** FFA, **f** proposed method

clear images to train the depth neural network model. A series of hazy images with different hazy levels are generated by setting different scattering coefficient  $\beta$  and atmospheric light intensity  $A$ . In this work, the RESIDE Dataset [27] is used to train the network model. The dataset includes Indoor Training Set (ITS), Outdoor Training Set (OTS) and Synthetic Objective Testing Set (SOTS). The ITS contains 1399 clear images, each of which corresponds to 10 foggy images with different hazy levels. The hazy images are generated according to  $\beta \in [0.6, 1.8]$  and  $A \in [0.7, 1.0]$ . The OTS contains 8790 clear images with their 35 corresponding hazy images of different levels, i.e., dataset size of  $8790 \times 35$ . The hazy images are generated according to  $\beta \in [0.04, 0.2]$  and  $A \in [0.8, 1.0]$ . The SOTS contains 500 indoor hazy images (TESTSET A) and 500 outdoor hazy images (TESTSET B). The synthesized hazy dataset in [25] is also used, and it con-

**Table 2** Comparison of running time with different dehazing methods

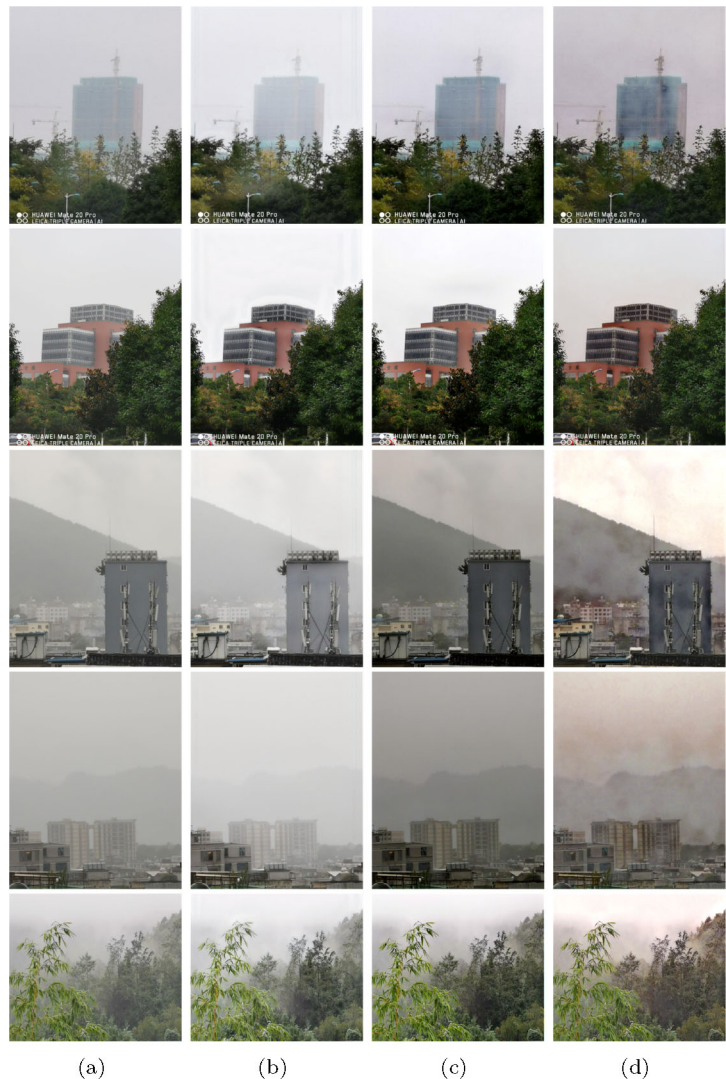
Metric	DCP	DA-Net	NLD	FFA-Net	Ours
Time (s)	0.61	1.63	1.72	0.95	0.91

tains 27,256 training images and 3170 non-overlapping test images (TESTSET C).

We use Pytorch plat for implementation. We utilize the U-net framework pretrained on clear images as our backbone for teacher network and use U-net framework without pretrained as student network. The network is trained with the RGB image patches size of  $480 \times 640$ . For the accelerated training, Adam optimizer is used with a batch size of 9. Batch normalization is not applied following [33,39]. The initial

**Table 3** Objective evaluation of ablation experiment

Methods	PSNR (dB)	SSIM
Baseline ( $L_{MSE} + L_p + L_c$ )	22.18	0.8533
$L_{MSE} + L_p + L_c + L_{\text{distill}}$	25.32	0.8978
$L_{MSE} + L_p + L_c + L_{\text{distill}} + L_{\text{TLD}} + L_{\text{LCD}}$	<b>27.38</b>	<b>0.9182</b>

**Fig. 5** Comparison of experimental results with different methods. **a** Source, **b** baseline, **c** baseline plus distillation loss, **d** baseline plus distillation loss and dual adversarial loss

learning rate is set to 0.0001. For ITS, we train the network for 100 epochs in total and the learning rate decreased by the poly policy [50]. As for OTS, the network is trained only for 10 epochs [35] and the learning rate also decreased by the poly policy. We set  $\lambda_1 = 0.001$  and  $\lambda_2 = 0.0015$ . The training is carried out on a terminal with GPU NVIDIA GeForce GTX 2080Ti.

Then, we evaluate the proposed method on both synthetic hazy images and real scene hazy images, and compare the performance with the state-of-the-art methods.

### 4.3 Experiments on synthetic datasets

Three synthetic datasets (TESTSET A, B and C) are used to evaluate the performance of the proposed method. The results are compared with state-of-the-art dehazing algorithms including DCP [16], NLD [3], DA-Net [46] and DehazeNet [4]. Figure 2 shows the dehazing results of the proposed method on synthetic hazy images.

The first row shows the hazy images, the second row shows the corresponding dehazing results with the proposed method, and the third row is the corresponding haze-free

images. It can be seen that the dehazing results of 1st, 5th and 8th column are satisfactory while the remaining have relatively poor dehazing effects. The fact is that the poor results are from the images with heavy haze. The dehazing results from different methods on the synthetic hazy images are shown in Fig. 3.

As shown in Fig. 3, DCP, NLD and DehazeNet suffer from color distortion in some cases. The results produced by DCP, NLD and DA-Net are over-enhanced and unrealistic. The proposed method restores images with a better visual effect and is most similar to the ground truth.

To further verify the effectiveness of the proposed method, PSNR and SSIM are used to measure the quality of the dehazing results. The larger value of PSNR and SSIM indicates better quality of the dehazed image. Quantitative assessments of all comparative methods are performed on TESTSET A, B and C. The average PSNR and SSIM results on TESTSET A, B and C are presented in Table 1 with the optimal values highlighted in bold.

As shown in Table 1, the proposed method outperforms other methods compared in this section and the experimental results confirms its dehazing ability visually (see Fig. 3). Therefore, it can be concluded that the proposed method delivers the best performance in terms of both subjective and objective evaluation.

#### 4.4 Experiments on real scene hazy images

To evaluate the feasibility of the proposed method, it is thus implemented on hazy images collected in the real world, and the results are compared with other methods including DCP [16], NLD [3], DA-Net [46] and FFA-Net [41]. Figure 4 shows the dehazing results of different methods applied to real scene hazy images. It can be seen that DCP, NLD and DA-Net suffer from serious color distortion. Although FFA-Net has achieved a better visual, its dehazing performance, on the other hand, is worse than the proposed method. It thus can be concluded that the proposed method outperforms the methods tested in terms of dehazing for real scene images. However, the dehazing effect of the proposed method on real hazy images is still unsatisfactory and is expected to be further improved.

Then, we compare the computational efficiency of the proposed method with other aforementioned methods by Pytorch on a terminal with GPU NVIDIA GeForce GTX 2080Ti. The running times of dehazing a  $1920 \times 1440$  pixels image with different methods are shown in Table 2. It can be seen that the computational efficiency of the proposed method ranks the second among all methods, and is superior to other deep learning-based methods such as DA-Net and FFA-Net.

#### 4.5 Ablation experiment

The ablation experiments are performed to verify the effectiveness of the proposed distillation loss ( $L_{\text{distill}}$ ) and dual adversarial loss ( $L_{\text{TLD}}$  and  $L_{\text{LCD}}$ ). Firstly, we train the U-Net student network with MSE loss, perceptual loss and color loss on TESTSET C, which is used as the baseline of the proposed dehazing network. Then, distillation loss and dual adversarial loss are added in turn. The evaluation results of these three networks are presented in Table 3. It can be seen that the PSNR and SSIM increase by 3.14 dB and 0.04, respectively, once the distillation loss is added. The PSNR and SSIM increase by 2.06 dB and 0.02, respectively, when the dual adversarial loss is added. Moreover, the visual effect of the ablation experiment on hazy images in real scene is shown in Fig. 5. It can be seen that the dehazing results are better once the distillation and the adversarial loss are added. It can be thus concluded that both distillation loss and dual adversarial loss contribute to the dehazing process.

#### 5 Conclusion

By examining the drawbacks of prior knowledge-based image dehazing methods and the problem of insufficient utilization of clear image labels, we present an end-to-end dehazing teacher–student stream based on the knowledge distillation. The feature maps of the clear haze-free image extracted by the TS are used to guide the dehazing process in the SS. Moreover, a novel dual adversarial strategy is developed to boost up the ability of SS to imitate the TS. The experiment results confirm the effectiveness and the superiority of the proposed method and verify the effect of the distillation and dual adversarial strategy for dehazing. The improvement of the proposed method for thick hazy images could be expected in the future study.

**Acknowledgements** This work is partly supported by the Science and Technology Project of Yunnan Power Grid Co., Ltd. (No. YNKJXM 20190729) and the National Key Research and Development Plan Project (Nos. 2018YFC0830105 and 2018YFC0830100).

#### References

1. Algabri, M., Mathkour, H., Bencherif, M.A., Alsulaiman, M., Mekhtiche, M.A.: Towards deep object detection techniques for phoneme recognition. *IEEE Access* **8**, 54663–54680 (2020)
2. Ba, L.J., Caruana, R.: Do deep nets really need to be deep? In: *Proceedings of the 27th International Conference on Neural Information Processing Systems*, vol 2, pp 2654–2662 (2014)
3. Berman, D., Treibitz, T., Avidan, S.: Non-local image dehazing. In: *2016 IEEE Conference on Computer Vision and Pattern Recognition (CVPR)*, pp. 1674–1682. Las Vegas, NV (2016)

4. Cai, B., Xu, X., Jia, K., Qing, C., Tao, D.: Dehazenet: an end-to-end system for single image haze removal. *IEEE Trans. Image Process.* **25**(11), 5187–5198 (2016)
5. Chen, D., He, M., Fan, Q., Liao, J., Zhang, L., Hou, D., Yuan, L., Hua, G.: Gated context aggregation network for image dehazing and deraining. In: *IEEE Winter Conference on Applications of Computer Vision (WACV)*, pp. 1375–1383. IEEE (2019)
6. Chen, J., Chen, J., Chao, H., Yang, M.: Image blind denoising with generative adversarial network based noise modeling. In: *2018 IEEE/CVF Conference on Computer Vision and Pattern Recognition*, pp. 3155–3164. IEEE, Salt Lake City, UT (2018)
7. Chen, Z., Hu, Z., Sheng, B., Li, P., Kim, J., Wu, E.: Simplified non-locally dense network for single-image dehazing. *Vis. Comput.* **36**(2), 2189–2200 (2020)
8. Choi, L.K., You, J., Bovik, A.C.: Referenceless prediction of perceptual fog density and perceptual image defogging. *IEEE Trans. Image Process.* **24**(11), 3888–3901 (2015)
9. Dong, Y., Liu, Y., Zhang, H., Chen, S., Qiao, Y.: Fd-gan: generative adversarial networks with fusion-discriminator for single image dehazing. [arXiv:2001.06968](https://arxiv.org/abs/2001.06968) (2020)
10. Engin, D., Genc, A., Ekenel, H.K.: Cycle-dehaze: enhanced cycle-gan for single image dehazing. In: *2018 IEEE/CVF Conference on Computer Vision and Pattern Recognition Workshops (CVPRW)*, pp. 938–9388. IEEE, Venice (2018)
11. Feng, J., Wu, X., Chen, J., Zhang, X., Tang, X., Li, D.: Joint multi-layer spatial-spectral classification of hyperspectral images based on CNN and convlstm. In: *IGARSS 2019–2019 IEEE International Geoscience and Remote Sensing Symposium*, pp. 588–591. IEEE, Japan (2019)
12. Ge, S., Zhao, S., Li, C., Li, J.: Low-resolution face recognition in the wild via selective knowledge distillation. *IEEE Trans. Image Process.* **28**(4), 2051–2062 (2019)
13. Ge, S., Zhao, S., Li, C., Zhang, Y., Li, J.: Efficient low-resolution face recognition via bridge distillation. *IEEE Trans. Image Process.* **29**(4), 6898–6980 (2020)
14. Guo, F., Zhao, X., Tang, J., Huipeng, L.L., Zou, B.: Single image dehazing based on fusion strategy. *Neurocomputing* **378**, 9–23 (2020)
15. Ha, E., Lim, H., Yu, S., Paik, J.: Low-light image enhancement using dual convolutional neural networks for vehicular imaging systems. In: *2020 IEEE International Conference on Consumer Electronics (ICCE)*, pp. 1–2. IEEE, Las Vegas, NV (2020)
16. He, K., Sun, J., Tang, X.: Single image haze removal using dark channel prior. *IEEE Trans. Pattern Anal. Mach. Intell.* **33**(12), 2341–2353 (2011)
17. Heo, B., Kim, J., Yun, S., Park, H., Kwak, N., Choi, J.Y.: A comprehensive overhaul of feature distillation. In: *2019 IEEE/CVF International Conference on Computer Vision (ICCV)*, pp. 1921–1930. IEEE, Seoul, Korea (South) (2019)
18. Hinton, G., Vinyals, O., Dean, J.: Distilling the knowledge in a neural network. [arXiv:1503.02531](https://arxiv.org/abs/1503.02531) (2015)
19. Hong, M., Xie, Y., Li, C., Qu, Y.: Distilling image dehazing with heterogeneous task imitation. In: *2020 IEEE/CVF Conference on Computer Vision and Pattern Recognition (CVPR)*, pp. 3459–3468. IEEE, Seattle (2020)
20. Ignatov, A., Kobyshev, N., Timofte, R., Vanhoey, K.: DSLR-quality photos on mobile devices with deep convolutional networks. In: *2017 IEEE International Conference on Computer Vision (ICCV)*, pp. 3297–3305. IEEE, Venice (2017)
21. Justin, J., Alexandre, A., Li, F.F.: Perceptual losses for real-time style transfer and super-resolution. In: *2016 European Conference on Computer Vision (ECCV)*, pp. 694–711 (2016)
22. Khmag, A., Al-Haddad, S.A.R., Ramli, A.R., Kalantar, B.: Single image dehazing using second-generation wavelet transforms and the mean vector l2-norm. *Vis. Comput.* **34**(5), 675–688 (2018)
23. Kupyn, O., Budzan, V., Mykhailych, M., Mishkin, D., Matas, J.: Deblurgan: blind motion deblurring using conditional adversarial networks. In: *2018 IEEE/CVF Conference on Computer Vision and Pattern Recognition*, pp. 8183–8192. IEEE, Salt Lake City, UT (2018)
24. Ledig, C., Theis, L., Huszar, F., Caballero, J., Cunningham, A., Acosta, A., Aitken, A., Tejani, A., Totz, J., Wang, Z., Shi, W.: Photo-realistic single image super-resolution using a generative adversarial network. In: *2017 IEEE Conference on Computer Vision and Pattern Recognition (CVPR)*, pp. 105–114. IEEE, Honolulu, HI (2017)
25. Li, B., Peng, X., Wang, Z., Xu, J., Feng, D.: An all-in-one network for dehazing and beyond. *ICCV* **2017**, 4770–4778 (2017a)
26. Li, B., Peng, X., Wang, Z., Xu, J., Feng, D.: Aod-net: All-in-one dehazing network. In: *2017 IEEE International Conference on Computer Vision (ICCV)*, pp. 4780–4788 (2017b)
27. Li, B., Ren, W., Fu, D., Tao, D., Feng, D., Zeng, W., Wang, Z.: Benchmarking single-image dehazing and beyond. *IEEE Trans. Image Process.* **28**(1), 492–505 (2019)
28. Li, H., He, X., Tao, D., Tang, Y., Wang, R.: Joint medical image fusion, denoising and enhancement via discriminative low-rank sparse dictionaries learning. *Pattern Recognit.* **79**, 130–146 (2018a)
29. Li, H., He, X., Yu, Z., Luo, J.: Noise-robust image fusion with low-rank sparse decomposition guided by external patch prior. *Inf. Sci.* **523**, 14–37 (2020a)
30. Li, H., Wang, Y., Yang, Z., Wang, R., Li, X., Tao, D.: Discriminative dictionary learning-based multiple component decomposition for detail-preserving noisy image fusion. *IEEE Trans. Instrum. Meas.* **69**(4), 1082–1102 (2020b)
31. Li, Q., Bi, D., Xu, Y., Zha, Y.: Haze degraded image scene rendition. *Acta Autom. Sin.* **40**(4), 744–750 (2014)
32. Li, R., Pan, J., Li, Z., Tang, J.: Single image dehazing via conditional generative adversarial network. In: *2018 IEEE/CVF Conference on Computer Vision and Pattern Recognition*, pp. 8202–8211. Salt Lake City, UT (2018b)
33. Lim, B., Son, S., Kim, H., Nah, S., Lee, K.M.: Enhanced deep residual networks for single image super-resolution. In: *2017 IEEE Conference on Computer Vision and Pattern Recognition Workshops (CVPRW)*, pp. 1132–1140. IEEE, Honolulu, HI (2017)
34. Liu, R., Fan, X., Hou, M., Jiang, Z., Luo, Z., Zhang, L.: Learning aggregated transmission propagation networks for haze removal and beyond. *IEEE Trans. Neural Netw. Learn. Syst.* **30**(10), 2973–2986 (2019a)
35. Liu, X., Ma, Y., Shi, Z., Chen, J.: Griddehazenet: attention-based multi-scale network for image dehazing. In: *2019 IEEE/CVF International Conference on Computer Vision (ICCV)*, pp. 7313–7322. IEEE, Seoul (2019b)
36. Mannos, J., Sakrison, D.: The effects of a visual fidelity criterion of the encoding of images. *IEEE Trans. Inf. Theory* **20**(4), 525–536 (1974)
37. Mehta, A., Sinha, H., Narang, P., Mandal, M.: Hidegan: A hyperspectral-guided image dehazing gan. In: *The IEEE/CVF Conference on Computer Vision and Pattern Recognition Workshops (CVPRW)*, pp. 846–856 (2020)
38. Meng, G., Wang, Y., Duan, J., Xiang, S., Pan, C.: Efficient image dehazing with boundary constraint and contextual regularization. In: *2013 IEEE International Conference on Computer Vision (ICCV)*, pp. 617–624. NSW, Sydney (2013)
39. Nah, S., Kim, T.H., Lee, K.M.: Deep multi-scale convolutional neural network for dynamic scene deblurring. In: *2017 IEEE Conference on Computer Vision and Pattern Recognition (CVPR)*, pp. 257–265. IEEE, Honolulu, HI (2017)
40. Pan, Y., He, F., Yu, H.: A novel enhanced collaborative auto-encoder with knowledge distillation for top-n recommender systems. *Neurocomputing* **332**, 137–148 (2019)

41. Qin, X., Wang, Z., Bai, Y., Xie, X.: FFA-net: feature fusion attention network for single image dehazing. *Proc. AAAI Conf. Artif. Intell.* **34**, 11908–11915 (2020)
42. Ren, W., Liu, S., Zhang, H., Pan, J., Cao, X., Yang, M.H.: Single image dehazing via multi-scale convolutional neural networks. In: 2016 European Conference on Computer Vision (ECCV), vol. 9906, pp. 154–169 (2016)
43. Ren, W., Ma, L., Zhang, J., Pan, J., Cao, X., Liu, W., Yang, M.H.: Gated fusion network for single image dehazing. In: 2018 IEEE/CVF Conference on Computer Vision and Pattern Recognition, pp. 3253–3261. Salt Lake City, UT (2018)
44. Romero, A., Ballas, N., Kahou, S.E., Chassang, A., Gatta, C., Bengio, Y.: Fitnets: hints for thin deep nets. [arXiv:1412.6550](https://arxiv.org/abs/1412.6550) (2014)
45. Ronneberger, O., Fischer, P., Brox, T.: U-net: Convolutional networks for biomedical image segmentation. In: *Medical Image Computing and Computer-Assisted Intervention—MICCAI 2015*, pp. 234–241. Springer International Publishing (2015)
46. Shao, Y., Li, L., Ren, W., Gao, C., Sang, N.: Domain adaptation for image dehazing. In: 2020 IEEE/CVF Conference on Computer Vision and Pattern Recognition (CVPR), pp. 2805–2814. IEEE, Seattle (2020)
47. Song, Y., Li, J., Wang, X., Chen, X.: Single image dehazing using ranking convolutional neural network. *IEEE Trans. Multimed.* **20**(6), 1548–1560 (2018)
48. Swami, K., Das, S.K.: Candy: Conditional adversarial networks based fully end-to-end system for single image haze removal. In: 2018 24th International Conference on Pattern Recognition (ICPR), pp. 3061–3067. Beijing (2018)
49. Tang, G., Zhao, L., Jiang, R., Zhang, X.: Single image dehazing via lightweight multi-scale networks. In: 2019 IEEE International Conference on Big Data (Big Data), pp. 5062–5069. IEEE, Los Angeles, CA (2019)
50. Tong, S., Dong, G., Wei, Z., Chunhua, S., Tao, M.: Regularizing proxies with multi-adversarial training for unsupervised domain-adaptive semantic segmentation. [arXiv:1907.12282](https://arxiv.org/abs/1907.12282) (2019)
51. Wang, J.B., He, N., Zhang, L.L., Lu, K.: Single image dehazing with a physical model and dark channel prior. *Neurocomputing* **149**, 718–728 (2015)
52. Wang, Z., Bovik, A.C., Sheikh, H.R., Simoncelli, E.P.: Image quality assessment: from error visibility to structural similarity. *IEEE Trans. Image Process.* **13**(4), 600–612 (2004)
53. Wu, H., Liu, J., Xie, Y., Qu, Y., Ma, L.: Knowledge transfer dehazing network for nonhomogeneous dehazing. In: 2020 IEEE/CVF Conference on Computer Vision and Pattern Recognition Workshops (CVPRW), pp. 1975–1983. IEEE, Seattle (2020)
54. Xie, M., Zhou, Z., Zhang, Y.: Joint framework for image fusion and super-resolution via multicomponent analysis and residual compensation. *IEEE Access* **7**, 174092–174107 (2019)
55. Yang, C., Xie, L., Qiao, S., Yuille, A.: Knowledge distillation in generations: more tolerant teachers educate better students. [arXiv:1805.05551](https://arxiv.org/abs/1805.05551) (2018a)
56. Yang, D., Sun, J.: Proximal dehaze-net: a prior learning-based deep network for single image dehazing. In: 2018 European Conference on Computer Vision, vol. 11211, pp. 729–746 (2018)
57. Yang, F., Zhang, Q.: Depth aware image dehazing. *Vis. Comput.* <https://doi.org/10.1007/s00371-021-02089-3> (2021)
58. Yang, X., Xu, Z., Luo, J.: Towards perceptual image dehazing by physics-based disentanglement and adversarial training. In: 2018 AAAI, New Orleans, pp. 7478–7485 (2018b)
59. Yim, J., Joo, D., Bae, J., Kim, J.: A gift from knowledge distillation: Fast optimization, network minimization and transfer learning. In: 2017 IEEE Conference on Computer Vision and Pattern Recognition (CVPR), pp. 7130–7138. IEEE, Honolulu, HI (2017)
60. Zagoruyko, S., Komodakis, N.: Paying more attention to attention: improving the performance of convolutional neural networks via attention transfer. In: 5th International Conference on Learning Representations, ICLR 2017 (2017)
61. Zhang, H., Patel, V.M.: Densely connected pyramid dehazing network. In: 2018 IEEE/CVF Conference on Computer Vision and Pattern Recognition, pp. 3194–3203. Salt Lake City, UT (2018)
62. Zhang, H., Sindagi, V., Patel, V.M.: Image de-raining using a conditional generative adversarial network. *IEEE Trans. Circ. Syst. Video Technol.* 1–1 (2019a)
63. Zhang, J., Cao, Y., Wang, Y., Wen, C., Chen, C.W.: Fully point-wise convolutional neural network for modeling statistical regularities in natural images. In: 2018 ACM Multimedia Conference (2018)
64. Zhang, S., He, F.: Drcdn: learning deep residual convolutional dehazing networks. *Vis. Comput.* <https://doi.org/10.1007/s00371-019-01774-8> (2020)
65. Zhang, S., He, F., Ren, W.: NLDN: non-local dehazing network for dense haze removal. *Neurocomputing* **410**, 363–373 (2020a)
66. Zhang, S., He, F., Ren, W., Yao, J.: Joint learning of image detail and transmission map for single image dehazing. *Vis. Comput.* **36**(2), 305–316 (2020b)
67. Zhang, W., Liu, Y., Dong, C., Qiao, Y.: Rankrgan: generative adversarial networks with ranker for image super-resolution. In: 2019 IEEE/CVF International Conference on Computer Vision (ICCV), pp. 3096–3105. IEEE, Seoul, Korea (South) (2019b)
68. Zhang, Y., Yang, M., Li, N., Yu, Z.: Analysis-synthesis dictionary pair learning and patch saliency measure for image fusion. *Signal Process.* **167**, 107327 (2020c)
69. Zheng, M., Qi, G., Zhu, Z., Li, Y., Wei, H., Liu, Y.: Image dehazing by an artificial image fusion method based on adaptive structure decomposition. *IEEE Sens. J.* **20**(4), 8062–8072 (2020)
70. Zhu, J.Y., Park, T., Isola, P., Efros, A.A.: Unpaired image-to-image translation using cycle-consistent adversarial networks. In: 2017 IEEE International Conference on Computer Vision (ICCV), pp. 2242–2251. IEEE, Venice (2017)
71. Zhu, Z., Wei, H., Hu, G., Li, Y., Qi, G., Mazur, N.: A novel fast single image dehazing algorithm based on artificial multi-exposure image fusion. *IEEE Trans. Instrum. Meas.* (2020). <https://doi.org/10.1109/TIM.2020.3024335>

**Publisher's Note** Springer Nature remains neutral with regard to jurisdictional claims in published maps and institutional affiliations.



**Zhengyun Fang** is currently pursuing a Ph.D. degree at Kunming University of Science and Technology. His main research interests include pattern recognition and image processing.



**Ming Zhao** is currently a professor at Electric Power Research Institute of Yunnan Power Grid Co., Ltd.. His main research interests include pattern recognition and power image processing.



**Meiyu Li** is currently an engineer at Electric Power Research Institute of Yunnan Power Grid Co., Ltd.. Her main research interests include pattern recognition and power image processing.



**Zhengtao Yu** Received his Ph.D. degree in computer application technology from Beijing Institute of Technology, Beijing, China, in 2005. He is currently a professor with the School of Information Engineering and Automation, Kunming University of Science and Technology, China. His main research interests include natural language process, image processing and machine learning.



**Yong Yang** is currently an assistant engineer at Electric Power Research Institute of Yunnan Power Grid Co., Ltd.. His main research interests include pattern recognition and power grid informatization.